states, as discussed above for $Fe^{III}TPP(Cl)$ and analogous pentacoordinate complexes.

Acknowledgment. This work was supported in part by National Institutes of Health Grant AM 30479 (D.W.D.) and by BRSG S07RR7054-17 awarded by the Biomedical Research Grant Program, Division of Research Resources, National Institutes of Health (D.H.).

Registry No. $Fe^{III}TPP(Cl)$, 16456-81-8; $Fe^{II}TPP(pip)_2$, 17845-65-7; $Fe^{II}TPP(1\text{-}MeIm)_2$, 54032-54-1; $Fe^{II}TPP(2\text{-}MeIm)$, 48243-44-3; $Fe^{II}PPDME(pip)_2$, 57300-83-1; $Fe^{II}DPDME(pip)_2$, 94203-24-4.

Copper Carbonyls, Cu(CO) and $Cu(CO)_3$: Matrix Isolation ESR Study

Paul H. Kasai* and Paul M. Jones

Contribution from IBM Instruments, Inc., Orchard Park, Danbury, Connecticut 06810.
Received August 16, 1984

Abstract: ESR spectra of copper carbonyls, Cu(CO) and $Cu(CO)_3$, generated in argon matrices were observed and analyzed. The g tensors and the hyperfine coupling tensors of the Cu and ^{13}C nuclei in each complex were determined. The $Cu(CO)_3$ spectra were complicated by forbidden transitions induced by severe anisotropy of the hyperfine coupling tensor and the nuclear quadrupole interaction of the Cu nucleus; the effect was demonstrated and the quadrupole interaction tensor was determined. Both carbonyls are formed by a σ-type dative interaction between the lone-pair electrons of CO and vacant hybrid sp orbital(s) of Cu and π-type back-donation from the Cu atom to the vacant π^* orbitals of the CO moiety. In Cu(CO) the back-donation is from the filled d_π orbitals, and the semifilled orbital is an sp_σ orbital of Cu pointing away from the ligand. $Cu(CO)_3$ is trigonal planar, and the back-donation results from interaction of the semifilled p_π orbital of Cu with the vacant π^* orbitals of CO molecules.

Introduction

The stability of mononuclear transition metal carbonyls such as $Cr(CO)_6$ or $Ni(CO)_4$ is well known. The bonding scheme of these complexes invokes a σ-type dative interaction of the lone-pair electrons of CO with the vacant valence orbitals of the metal atom, and π-type back-donation from the filled d_π orbitals of the metal atom to the vacant π^* orbitals of CO molecules.[1] Thermally stable carbonyls of the group 1B metal atoms (Cu, Ag, and Au), however, are not known. It is ascribed to the extra stability of the completed nd^{10} configuration of these atoms.

Ogden,[2] earlier, and Ozin and his co-workers,[3] later, showed that mononuclear carbonyls of group 1B metal atoms were formed when the metal atoms and CO molecules were cocondensed in rare gas matrices at cryogenic temperature (~4–20 K). A thorough analysis of vibrational spectra of the Cu/CO/Ar system by Ozin et al.[3] revealed the formation of Cu(CO), $Cu(CO)_2$, and $Cu(CO)_3$. It also showed that $Cu(CO)_2$ was linear, while $Cu(CO)_3$ was trigonal planar. In a separate paper Ozin reported on ESR (electron spin resonance) spectra of $Cu(CO)_3$ with a preliminary analysis, and a brief reference to an ESR spectrum of Cu(CO).[4] $Cu(CO)_2$ of a linear structure would have a $^2\Pi$ ground state, and its ESR spectrum would not be observed.

Accurate descriptions of the semifilled orbitals of these complexes, if obtained, should be extremely elucidative of the structures and bonding schemes involved. We report here ESR spectra of copper carbonyls observed from the Cu/CO/Ar system, and their detailed analyses. The g tensors and the hfc (hyperfine coupling) tensors with the Cu and ^{13}C nuclei of Cu(CO) and $Cu(CO)_3$ were determined. As expected no ESR signal attributable to $Cu(CO)_2$ was observed. It is shown that the semifilled orbital of Cu(CO) is a hybrid sp_σ orbital of Cu pointing away from the ligand, while the semifilled orbital of $Cu(CO)_3$ represents the back-donation from the Cu $4p_\pi$ orbital into the π^* orbitals of CO molecules.

Experimental Section

A liquid helium cryostat that would enable trapping of vaporized metal atoms in an inert gas matrix and examination of the resulting matrix by ESR has been described earlier.[5] In the present series of experiments, copper atoms were generated from a resistively heated (~1400 °C) tantalum cell and were trapped in argon matrices containing a controlled amount of carbon monoxide (~1–4%).

The ESR spectrometer used was an IBM Model ER200D system, and a low-frequency (375 Hz) field modulation was used for the signal detection. All the spectra reported here were obtained while the matrix was maintained at ~4 K. The spectrometer frequency locked to the sample cavity was 9.4250 GHz and a typical microwave power level was ~5 μW.

Research grade argon and CP grade carbon monoxide were obtained from Matheson, and ^{13}C-enriched (enrichment >90%) carbon monoxide was obtained from MSD Isotopes.

Results

The ESR spectrum of Cu atoms ($3d^{10}4s^1$) isolated in rare gas matrices has already been analyzed.[6] There are two naturally abundant Cu isotopes, ^{63}Cu (natural abundance = 69%, $I = 3/2$, $\mu = 2.2206\beta_n$) and ^{65}Cu (natural abundance = 31%, $I = 3/2$, $\mu = 2.3790\beta_n$). Owing to the large hfc interaction with those nuclei, the ESR spectrum of Cu atoms observed with an X-band spectrometer shows only two resonance transitions; one corresponds to the "NMR" transition ($M_S = {}^1/_2$, $M_I = -{}^1/_2 \leftrightarrow -{}^3/_2$) and occurs at 1.5 and 2.0 kG for ^{63}Cu and ^{65}Cu, respectively, and the other corresponds to the ESR transition ($M_S = -{}^1/_2 \leftrightarrow +{}^1/_2$, $M_I = -{}^3/_2$), and occurs at 5.8 and 6.0 kG.

Figure 1 shows the ESR spectrum observed from the Cu/CO-(2%)/Ar system. Three types of signals A, B, and C are indicated. The signals A are those of isolated Cu atoms described above. The signals B and C were observed only when Cu and CO were cocondensed. When the CO concentration was low (~1%), the A and B signals dominated the spectrum, and, when the CO concentration was high (~4%), the C signals were the most dominant. The color of the argon matrix changed from pale blue to purple with increasing CO concentration. Thus, based on these observations and in cognizance of conclusions reached in the IR

(1) See, for example: Cotton, F. A.; Wilkinson, G. "Advanced Inorganic Chemistry", 4th ed.; Wiley: New York, 1980; pp 82–86, 1049–1079.
(2) Ogden, J. S. *J. Chem. Soc., Chem. Commun.* **1971**, 978.
(3) Huber, H.; Künding, E. P.; Moskovits, M.; Ozin, G. A. *J. Am. Chem. Soc.* **1975**, *97*, 2097.
(4) Ozin, G. A. *Appl. Spectrosc.* **1976**, *30*, 573.
(5) Kasai, P. H. *Acc. Chem. Res.* **1971**, *4*, 329.
(6) Kasai, P. H.; McLeod, D., Jr. *J. Chem. Phys.* **1971**, *55*, 1566.

0002-7863/85/1507-0813$01.50/0

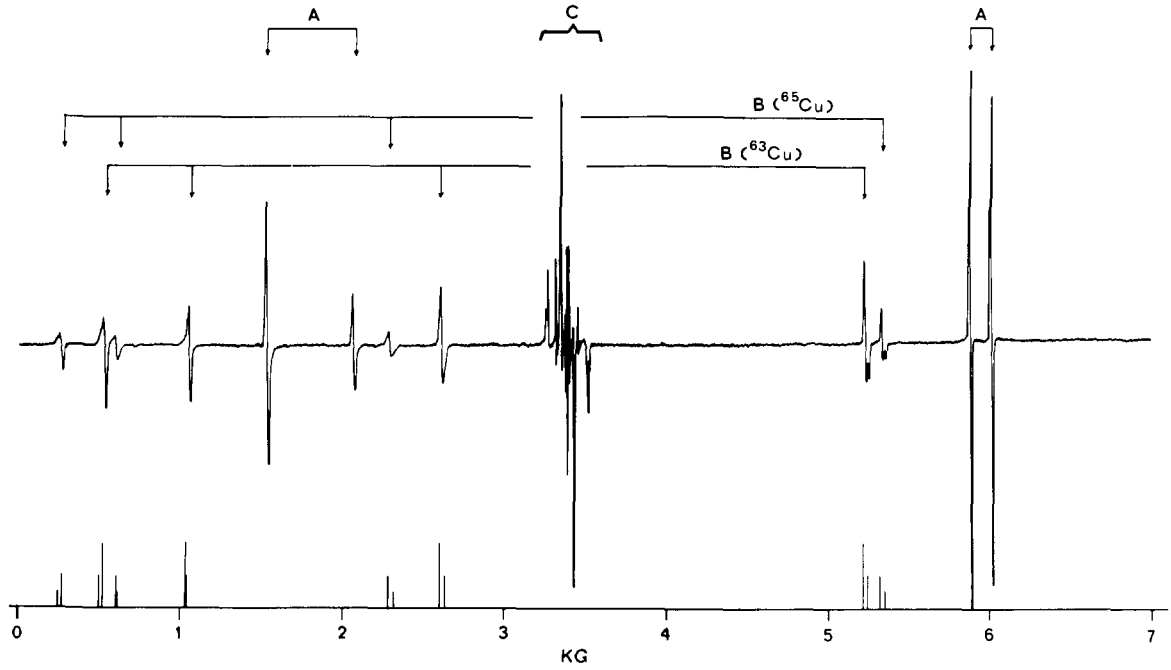

Figure 1. ESR spectrum observed from the Cu/CO (2%)/Ar system. Three types of signals A, B, and C are indicated. The bars at the bottom indicate the resonance positions of the B signals computed based on parameters given in the text.

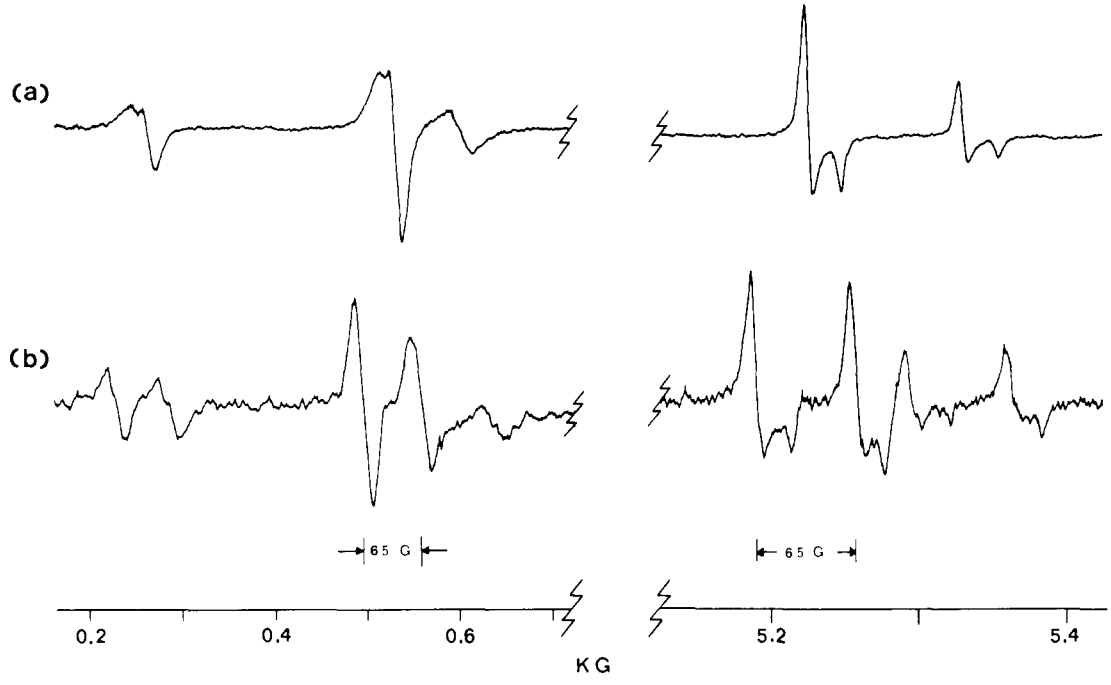

Figure 2. Spectral sections showing the lowest and the highest field components ($M_I = \pm^3/_2$) of B signals observed from (a) the Cu/CO (2%)/Ar system and (b) the Cu/^{13}CO (2%)/Ar system.

study of Ozin et al., the B signals were assigned to Cu(CO) and the C signals to $Cu(CO)_3$. Analyses of the individual spectra are presented below.

ESR Spectra of Cu(CO). As indicated in Figure 1, the B signals can be readily recognized as two sets of quartets arising from the hfc interactions with ^{63}Cu and ^{65}Cu. The highest and the lowest field components ($M_I = \pm^3/_2$) of the quartets are shown in Figure 2a in an expanded scale. The line shapes of these signals are clearly those expected from an ensemble of randomly oriented radicals having axially symmetric g and hfc tensors.[7] The observed parallel and perpendicular resonance fields of all the B signals are listed in Table I.

(7) For analyses of ESR powder pattern spectra see, for example: Ayscough, P. B. "Electron Spin Resonance in Chemistry"; Methuen: London, 1967; pp 323–332.

Table I. Observed Resonance Positions of Cu(CO) Generated in Argon Matrices[a]

isotopic species	hyperfine component (M_I)			
	+3/2	+1/2	−1/2	−3/2
^{63}Cu(CO)	508.9 (∥)	1043 (∥,⊥)	2587 (⊥)	5188 (⊥)
	530.0 (⊥)		2619 (∥)	5213 (∥)
^{65}Cu(CO)	242.4 (∥)	596 (∥,⊥)	2259 (⊥)	5292 (⊥)
	264.2 (⊥)		2304 (∥)	5319 (∥)

[a] Given in gauss, accuracy ±2 G, microwave frequency = 9.425 GHz.

ESR spectra of Cu(CO) of a linear structure should be describable by an axially symmetric spin Hamiltonian of eq 1. Here $A_\parallel$ and $A_\perp$ represent the hfc tensor with the Cu nucleus. When the hfc interaction is of such magnitude as that encountered here,

$$\hat{H}_{spin} = g_{\parallel}\beta H_z S_z + g_{\perp}\beta(H_x S_x + H_y S_y) + A_{\parallel} I_z S_z + A_{\perp}(I_x S_x + I_y S_y) \quad (1)$$

the usual second-order solution of the matrix would not yield the correct resonance positions. However, it has been shown that the parallel and perpendicular resonance fields, $H_{\parallel}(m)$ and $H_{\perp}(m)$, of a hyperfine component ($M_I = m$) are given accurately by the following "continued fraction" expressions:[8]

$$H_{\parallel}(m) = H_{\parallel}^0 - mA_{\parallel}' - F_{\parallel} - G_{\parallel}$$
$$H_{\perp}(m) = H_{\perp}^0 - mA_{\perp}' - F_{\perp} - G_{\perp} \quad (2)$$

where

$$F_{\parallel} = \frac{D_{\parallel}^2[I(I+1) - m(m+1)]}{H_{\parallel}(m) + (m + \frac{1}{2})A_{\parallel}' + F_{\parallel}}$$

$$G_{\parallel} = \frac{D_{\parallel}^2[I(I+1) - m(m-1)]}{H_{\parallel}(m) + (m - \frac{1}{2})A_{\parallel}' + G_{\parallel}}$$

$$F_{\perp} = \frac{D_{\perp}^2[I(I-1) - m(m+1)]}{H_{\perp}(m) + (m + \frac{1}{2})A_{\perp}' + F_{\perp}}$$

$$G_{\perp} = \frac{D_{\perp}^2[I(I+1) - m(m-1)]}{H_{\perp}(m) + (m - \frac{1}{2})A_{\perp}' + G_{\perp}}$$

$$H_{\parallel}^0 = \frac{h\nu}{g_{\parallel}\beta},\ H_{\perp}^0 = \frac{h\nu}{g_{\perp}\beta},\ A_{\parallel}' = \frac{A_{\parallel}}{g_{\parallel}\beta},\ A_{\perp}' = \frac{A_{\perp}}{g_{\perp}\beta}$$

$$D_{\parallel} = \frac{A_{\perp}}{2g_{\parallel}\beta},\ D_{\perp} = \frac{1}{4g_{\perp}\beta}(A_{\parallel} + A_{\perp})$$

From the observed resonance positions of the $M_I = \pm^3/_2$ components and eq 2, the consistent set of g and hfc tensors can be readily determined through a computer-assisted iteration process. The g tensor and the hfc tensor of ^{63}Cu(CO) were thus determined as follows:

$$g_{\parallel} = 1.998\ (1) \qquad A_{\parallel}(^{63}\text{Cu}) = 4174\ (2)\ \text{MHz}$$
$$g_{\perp} = 1.995\ (1) \qquad A_{\perp}(^{63}\text{Cu}) = 4126\ (2)\ \text{MHz}$$

The resonance positions of ^{63}Cu(CO) and ^{65}Cu(CO) computed from eq 2 based upon these parameters and the known ratio of the nuclear magnetic moments of ^{63}Cu and ^{65}Cu are shown at the bottom of Figure 1. The short and long bars indicate the parallel and perpendicular components, respectively.

When the matrix was prepared using ^{13}C-enriched CO (enrichment > 90%), all the B signals appeared as a doublet separated by ~65 G. Figure 2b shows the $M_I = \pm^3/_2$ components of spectrum B observed from the Cu/^{13}CO(2%)/Ar system. Apparently the relevant ^{13}C hfc tensor is essentially isotropic. Thus the following assignment was made:

$$A_{\parallel}(^{13}\text{C}) \simeq A_{\perp}(^{13}\text{C}) = 65 \pm 5\ \text{G}$$

Observation of the hfc with one ^{13}C nucleus constitutes a strong support to the assignment of the B signals to Cu(CO).

ESR Spectra of Cu(CO)$_3$. Figure 3a shows, in an expanded scale, the C signal region of the spectrum observed from the Cu/CO (4%)/Ar system. Signals due to inadvertently formed formyl (HCO) radicals can be readily recognized.[9] The indicated quartet with the successive spacings of 83 G is exactly that reported and assigned earlier by Ozin as the "parallel components" of Cu(CO)$_3$.[4] Shapes, signs, and relative intensities of these signals are indeed those expected for the parallel components of a system

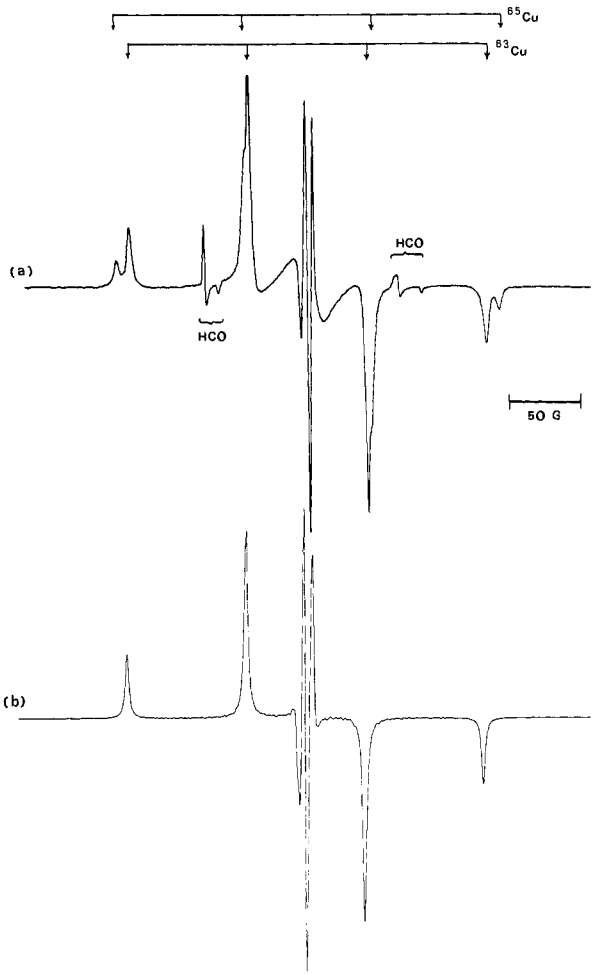

Figure 3. (a) The C signal region of the spectrum observed from the Cu/CO (4%)/Ar system. (b) Computer simulated spectrum based on parameters given in the text.

having a hfc tensor ($I = {}^3/_2$) of an extremely uniaxial nature ($A_{\parallel} >> A_{\perp}$). The central section of spectrum C shown here, however, does not have the signals observed and assigned earlier as the perpendicular components.[4] The only signals seen presently in this region are extremely sharp, closely spaced triplet of anomalous phases. In the earlier report, these signals were ascribed to impurities.[4]

The structure of Cu(CO)$_3$ has been established as being trigonal planar.[3] Its ESR spectrum might then be compatible with an axially symmetric spin Hamiltonian of the form given in eq 1. The symmetric appearance of the parallel components in Figure 3a dictates that the perpendicular components be within the innermost pair of these signals. They would surely be recognized as a regularly spaced quartet if $A_{\perp}$ were larger than the line width. Under no circumstances could they generate an isotropic signal at the center of the spectrum as the central component of the anomalous triplet. Computer simulation showed that there would be no discernible signal in the central region if $A_{\perp} = 0$.

It became apparent that the unique central feature should be ascribed to forbidden transitions $\Delta M_S = \pm 1$, $\Delta M_I = \pm 1$. It is well known that a nuclear quadrupole interaction can give rise to forbidden transitions where $\Delta M_S = \pm 1$ and $\Delta M_I = \pm 1$ or ± 2.[10] It has also been shown by McConnell et al. that forbidden transitions involving a nucleus of spin $^1/_2$ may occur if the hfc constant for a given orientation, the anisotropy of the hfc tensor, and the nuclear Zeeman term are all of similar magnitudes.[11] Let us examine an axially symmetric spin Hamiltonian appropriate for

(8) Kasai, P. H.; McLeod, D., Jr. *Faraday Discuss. Symp. 14*, **1980**, 65.
(9) Adrian, F. J.; Cochran, E. L.; Bowers, V. A. *J. Chem. Phys.* **1962**, *36*, 1661.
(10) Bleaney, B. *Phil. Mag.* **1951**, *42*, 441.
(11) McConnell, H. M.; Heller, C.; Cole, T.; Fessenden, R. W. *J. Am. Chem. Soc.* **1960**, *82*, 766.

$Cu(CO)_3$ including the nuclear quadrupole term, and the nuclear Zeeman term (eq 3).

$$\hat{H}_{spin} = g_{\parallel}\beta H_z S_z + g_{\perp}\beta(H_x S_x + H_y S_y) + A_{\parallel} S_z I_z + A_{\perp}(S_x I_x + S_y I_y) + Q[I_z^2 - \tfrac{1}{3}I(I+1)] - g_n\beta_n H \cdot I \quad (3)$$

Here Q represents an axially symmetric quadrupole interaction and g_n is the nuclear g factor. Transformation from molecular coordinates to laboratory coordinates following the scheme given by Bleaney[10] transforms eq 3 as follows:

$$\hat{H}_{spin} = g\beta H S_z + \hat{H}(A) + \hat{H}(Q) + \hat{H}(n) \quad (4a)$$

where

$$\hat{H}(A) = A S_z I_z + \left[\left(\frac{A_\perp^2 - A_\parallel^2}{A}\right)\times \left(\frac{g_\parallel g_\perp}{g^2}\right)\sin\theta\cos\theta\, S_x I_x + \frac{A_\perp}{4}\left(\frac{A_\parallel + A}{A}\right)(I_+S_- + I_-S_+) + \frac{A_\perp}{4}\left(\frac{A_\parallel - A}{A}\right)(I_+S_+ + I_-S_-)\right] \quad (4b)$$

$$\hat{H}(Q) = \frac{1}{2}Q\left[I_z^2 - \frac{1}{3}I(I+1)\right]\left[3\left(\frac{A_\parallel g_\parallel}{Ag}\right)^2\cos^2\theta - 1\right] - Q\frac{A_\parallel A_\perp g_\parallel g_\perp}{A^2 g^2}\cos\theta\sin\theta\,(I_z I_x + I_x I_z) + \frac{1}{4}Q\left(\frac{A_\perp g_\perp}{Ag}\right)^2\sin^2\theta\,(I_+^2 + I_-^2) \quad (4c)$$

$$\hat{H}(n) = -g_n\beta_n H\left(\frac{A_\parallel g_\parallel \cos^2\theta + A_\perp g_\perp \sin^2\theta}{Ag}\right)I_z - g_n\beta_n H\left(\frac{A_\parallel g_\parallel - A_\perp g_\perp}{Ag}\right)\sin\theta\cos\theta\, I_x \quad (4d)$$

Here θ is the angle between the magnetic field and the symmetry axis of the molecule, and g and A are defined in the usual manners.

$$g^2 = g_\parallel^2\cos^2\theta + g_\perp^2\sin^2\theta$$

$$A^2 = \left(\frac{A_\parallel g_\parallel}{g}\right)^2\cos^2\theta + \left(\frac{A_\perp g_\perp}{g}\right)^2\sin^2\theta$$

Hamiltonian matrix derived from eq 4a is diagonal with respect to the electronic Zeeman term $g\beta H \cdot S$. The only terms that would generate nonzero elements between the $M_S = \pm^1/_2$ blocks are those inside the brackets in eq 4b. These terms may be neglected if $g\beta H \cdot S >> A$.

Inspection of eq 4c reveals that, if $Q \simeq A$, the second and the third terms cause "mixing" of states differing in M_I by ± 1 and ± 2, respectively, within each M_S block. Inspection of eq 4d shows that, if A, $g_n\beta_n H$, and $A_\parallel - A_\perp$ are all of similar magnitudes, severe mixing occurs between states differing in M_I by ± 1 within each M_S block. Accurate assessment of the effect of these mixings under the stipulated conditions requires exact diagonalization of $(2I+1) \times (2I+1)$ matrices of each M_S blocks. Within each M_S block, the electronic Zeeman term $g\beta H S_z$ is common to all the diagonal elements, and thus can be removed from the diagonalization process. The magnetic field H associated with the nuclear Zeeman term (eq 4d) may be replaced by a "typical" field given by $h\nu/g\beta$. The two $(2I+1) \times (2I+1)$ matrices for $M_S = \pm^1/_2$ are now field independent and may be diagonalized for a given set of g, A, and Q tensors, and the field direction θ.

Let $E(+^1/_2,m)$ and $E(-^1/_2,m')$ be eigenvalues obtained by diagonalization of such matrices of $M_S = \pm^1/_2$, and let

$$\Phi_m^+ = \sum_{k=-I}^{+I} a_{km}|k\rangle \text{ and } \Phi_{m'}^- = \sum_{k=-I}^{+I} a_{km'}|k\rangle$$

Figure 4. Computer simulated C signals assuming the g and ^{63}Cu hfc tensors given in the text: (a) $Q = 0.00$, $g_n = 0.00$; (b) $Q = 2.00$ G, $g_n = 0.00$; (c) $Q = 0.00$, $g_n = 1.48$.

represent the corresponding eigenfunctions. Here $|k\rangle$ represents the nuclear spin state for which $M_I = k$. The ESR resonance field $H(m,m')$ and its transition probability $P(m,m')$ are then given by the following:

$$H(m,m') = \frac{h\nu}{g\beta} - E(+\tfrac{1}{2},m) + E(-\tfrac{1}{2},m') \quad (5a)$$

$$P(m,m') = [\sum_{k=-1}^{+I} a_{km}a_{km'}]^2 \quad (5b)$$

For the present case of $I = {}^3/_2$ there would formally be 16 transitions for each orientation. The algorithm employed above is that of Lund, Thuomas, and Maruani.[12] An ESR powder pattern simulation program of ours[13] was modified according to this scheme.

Using the modified program, effects of mixing of nuclear states by the nuclear quadrupole term and/or the nuclear Zeeman term were examined for the predicated situation $I = {}^3/_2$, $g_\parallel \simeq g_\perp = 2.00$, and $A_\parallel = 83.4$ G $>> A_\perp$. Several trial simulations revealed that the anomalous feature at the center of spectrum would not be produced if only the hyperfine term (eq 4b) are considered, nor when the hyperfine term and the quadrupole term (eq 4b and 4c) were considered (Figures 4a and 4b). However, when the hyperfine term and the nuclear Zeeman term (eq 4b and 4d) were considered, a very satisfactory result was obtained (Figure 4c).

A closer analysis of Figure 4c revealed that the outer components of the anomalous triplet were due to the outermost components of the "normal" perpendicular signals, while the sharp

(12) Lund, A.; Thuomas, K.; Maruani, J. *J. Magn. Reson.* **1978**, *30*, 505.
(13) Kasai, P. H. *J. Am. Chem. Soc.* **1972**, *94*, 5950.

Table II. g Tensors and ^{63}Cu and ^{13}C hfc Tensors (in MHz) of Cu(CO) and Cu(CO)$_3$

			^{63}Cu		^{13}C	
	$g_\parallel$	$g_\perp$	$A_\parallel$	$A_\perp$	$A_\parallel$	$A_\perp$
Cu(CO)	1.998 (1)	1.995 (1)	4174 (2)	4126 (2)	182 (6)	182 (6)
Cu(CO)$_3$	2.0008 (3)	2.0002 (3)	+233.5 (6)	−10 (1)	+6 (1)	−31 (2)

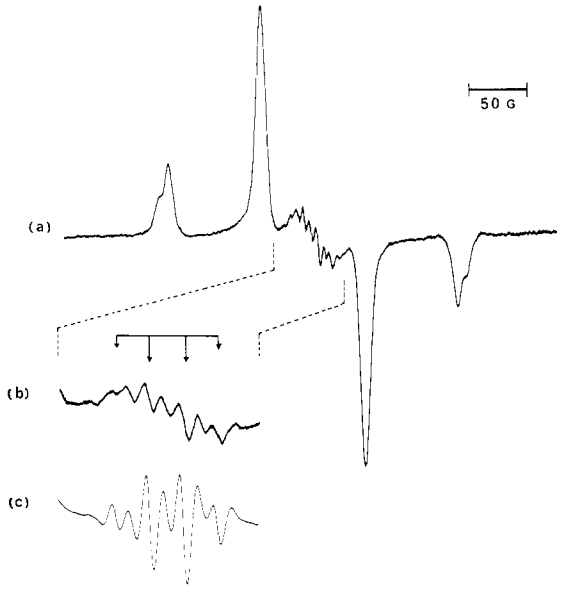

Figure 5. (a) The C signal region of the spectrum observed from the Cu/^{13}CO(4%)/Ar system. (b) the ⊥ region of (a) shown expanded. (c) The ⊥ region of simulated spectrum based on parameters given in the text.

central feature was due to forbidden transitions of the type $M_I = +^1/_2 \leftrightarrow -^1/_2$ in the $\theta = \sim 80$–$88°$ range. Also as seen in Figure 4c consideration of the hyperfine term and the nuclear Zeeman term alone always produced equally intense outer components of the anomalous triplet. The asymmetric intensity pattern for these peaks was produced when the quadrupole term was also considered. The following parameters were thus determined for ^{63}Cu(CO)$_3$:

$$g_\parallel = 2.0008\ (3),\ g_\perp = 2.0002\ (3),$$

$$A_\parallel(^{63}\text{Cu}) = 83.4\ (2)\ \text{G},\ A_\perp(^{63}\text{Cu}) = -3.5\ (5)\ \text{G},$$

$$Q(^{63}\text{Cu}) = 2.0\ (5)\ \text{G}$$

The simulated spectrum based upon these parameters is shown in Figure 3b. As expected the central section of the spectrum was particularly sensitive to $A_\perp$. If $A_\perp$ was changed to +3.5, the peak height of the anomalous triplet decreased reflecting a smaller value of $(A_\parallel - A_\perp)/A$ in eq 4d, and the asymmetry in the intensity of triplet was reversed.

Figure 5a shows the C signal region of the spectrum observed from the Cu/^{13}CO (4%)/Ar system. The hfc interaction with the ^{13}C nuclei broadens the parallel components and causes further splittings of the central signals. Hence $A_\parallel(^{13}\text{C})$ may be assessed from the line-width increase assuming the presence of three equivalent ^{13}C nuclei. Figure 5b shows, in an expanded scale, the central section of the ^{13}C-labeled spectrum. The 1:3:3:1 splitting of the central peak of the original triplet was recognized as indicated. The ^{13}C hfc tensor of Cu(CO)$_3$ was thus determined as follows:

$$|A_\parallel(^{13}\text{C})| = 2.0\ (2)\ \text{G and } |A_\perp(^{13}\text{C}) = 11.0\ (5)\ \text{G}$$

Figure 5c shows the central section of the spectrum simulated including the interaction with three equivalent ^{13}C nuclei of the hfc tensor given above. The discrepancy noted here, extra broadening of the observed peaks, is attributed to departure of the ^{13}C hfc tensor from axial symmetry. Observation of the hfc with three ^{13}C nuclei renders a strong support to the assignment of the C signals to Cu(CO)$_3$.

Discussion

The g tensors and the ^{63}Cu and ^{13}C hfc tensors of Cu(CO) and Cu(CO)$_3$ are listed in Table II. The hfc elements determined in gauss were converted to those in megahertz by multiplication by $g\beta$. Cu(CO) is expected to be linear. As stated earlier, Cu(CO)$_3$ has been shown to have a trigonal-planar structure by the IR study of Ozin and his co-workers.[3] The extremely large, essentially isotropic Cu hfc tensor in Cu(CO) indicates a large spin density in the Cu 4s orbital. The small, but extremely anisotropic Cu hfc tensor of Cu(CO)$_3$ indicates a substantial spin density in the Cu 4p orbital, but no "direct occupation" of the Cu 4s orbital by the unpaired electron. The most likely bonding schemes compatible with these observations were thus deduced as follows:

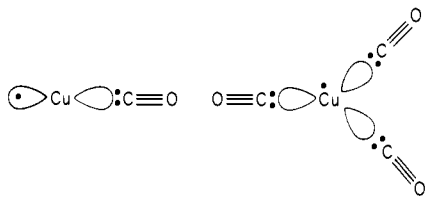

In each of these arrangements a σ-type dative interaction occurs between the lone-pair electrons of CO and vacant sp hybrid orbital(s) of the Cu atom, while π-type back-donation occurs from the Cu atom into the vacant π^* orbitals of CO. In Cu(CO) the back-donation is from the filled d_π orbitals, and the semifilled orbital is an sp_σ orbital of Cu pointing away from CO. The presence of back-donation is clearly indicated in the CO stretching frequency of Cu(CO).[3] In Cu(CO)$_3$ the back-donation is from th semifilled p_π orbital of Cu. The semifilled orbital of Cu(CO) and Cu(CO)$_3$ may thus be described as follows:

$$\Phi_1 = a\phi(4s)_{Cu} + b\phi(4p_\sigma)_{Cu} - c\phi(2s,2p_\sigma)_C \quad (6)$$

$$\Phi_3 = a\phi(4p_\pi)_{Cu} + b[\pi^*_1 + \pi^*_2 + \pi^*_3] \quad (7)$$

Here π^*_n represents the vacant π^* orbital of indicated CO. In eq 6 the term involving $\phi(2s,2p_\sigma)_C$ was included in order to make the orbital orthogonal to the orbital of the CO lone-pair electrons.

It has been shown that the principal elements, $A_\parallel$ and $A_\perp$, of an axially symmetric hfc tensor are related to the isotropic term A_{iso} and the anisotropic dipolar term A_{dip} as follows:[14]

$$A_\parallel = A_{iso} + 2A_{dip}$$

$$A_\perp = A_{iso} - A_{dip} \quad (8)$$

where

$$A_{iso} = g_e\beta_e g_n\beta_n \frac{8\pi}{3}\left|\Phi(0)\right|^2$$

$$A_{dip} = g_e\beta_e g_n\beta_n\left\langle\frac{3\cos^2\alpha - 1}{2r^3}\right\rangle = g_e\beta_e g_n\beta_n\frac{2}{5}\left\langle\frac{1}{r^3}\right\rangle_p$$

Here $|\Phi(0)|^2$ represents the spin density at the magnetic nucleus, r the separation between the nucleus and electron, and α the angle between r and the symmetry axis. Only the spin density in an s orbital contributes to A_{iso} and that in a non-s orbital to A_{dip}. The second expression for A_{dip} holds for a unit spin density in a p orbital of the magnetic nucleus.

Analyses of the observed ^{63}Cu hfc tensors in terms of eq 8 yield the following:

(14) See, for example: Atkins, P. W.; Symons, M. C. R. "The Structures of Inorganic Radicals"; Elsevier: Amsterdam, 1967; pp 14–20.

	A_{iso}	A_{dip}
Cu(CO)	4142 MHz	16 MHz
$Cu(CO)_3$	71 MHz	81 MHz

These values should be compared with the atomic values $A^0_{iso}(^{63}Cu)$ = 6151 MHz, the hfc constant of the ^{63}Cu atoms ($3d^{10}4s^1$) isolated in an argon matrix, and $A^0_{dip}(^{63}Cu)$ = 200 MHz, a value estimated for a unit spin density in the Cu 4p orbital from the known hf splitting term, $a(j = {}^1/_2)$, of the Ga atoms ($4s^24p^1$).[15] The atomic values A^0_{iso} and A^0_{dip} for the carbon 2s and 2p orbitals have been computed theoretically; they are $A^0_{iso}(^{13}C)$ = 3780 MHz, and $A^0_{dip}(^{13}C)$ = 107 MHz.[16] The observed ^{13}C hfc tensor of Cu(CO) is apparently dominated by the A_{iso} term. We thus assessed, from the observed hfc tensors, the following spin density distribution in Cu(CO): $\rho(4s)_{Cu} = +0.67$, $\rho(4p_\sigma)_{Cu} = +0.08$, and $\rho(2s)_C = +0.05$. The balance of spin density ($\sim$0.2) is believed to be mostly at the C $2p_\sigma$ orbital, and perhaps some at the oxygen $2p_\sigma$ and Cu $3d_\sigma$ orbitals.

In $Cu(CO)_3$ the ^{13}C hfc tensor is determined essentially by the C $2p_\pi$ orbital part of eq 7. The ^{13}C hfc tensor should thus be approximately axially symmetric, the symmetry axis being coincident with that of the Cu hfc tensor. For a positive spin density in a p orbital, A_{dip} in eq 8 is a positive quantity, and hence $A_\parallel > A_\perp$. We shall therefore assert, for the ^{13}C hfc tensor of $Cu(CO)_3$, $A_\parallel = +6$ MHz, and $A_\perp = -31$ MHz. Analysis of these quantities in terms of eq 8 yields $A_{iso}(^{13}C) = -18.7$ MHz and $A_{dip}(^{13}C) = +12.3$ MHz. We thus assessed the following spin density in $Cu(CO)_3$: $\rho(4s)_{Cu} = +0.01$, $\rho(2s)_C = -0.005$, $\rho(4p_\pi)_{Cu} = +0.41$, and $\rho(2p_\pi)_C = +0.11$. The small densities in the Cu 4s and C 2s orbitals are attributed to polarizations of filled orbitals. A negative spin density in the carbon 2s orbital is particularly interesting; it can be best accounted for by polarization of electrons in the σ dative bond by the large positive spin density in the Cu $4p_\pi$ orbital.

Recently we have observed and analyzed ESR spectra of $Al(CO)_2$ generated in argon matrices.[17] Its structure and bonding scheme were shown to be as follows:

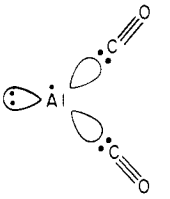

The aluminum complex is thus also formed by the σ-type dative interaction between the lone-pair electrons of CO and vacant sp hybrid orbitals of the metal atom and the back-donation from the semifilled p_π orbital of the metal atom. From the observed ^{27}Al and ^{13}C hfc tensors the following spin density distribution was assessed: $\rho(3s)_{Al} = +0.02$, $\rho(2s)_C = -0.004$, $\rho(3p_\pi)_{Al} = +0.42$, and $\rho(2p_\pi)_C = +0.09$. Similarity between the semifilled orbitals of $Cu(CO)_3$ and $Al(CO)_2$ is striking. The observed CO stretching frequencies of these complexes are also similar (1890 and 1988 cm^{-1} for the Al complex, and 1977 and 1990 cm^{-1} for the Cu complex). Noting that the $d_\pi \rightarrow \pi^*$ back-donation is impossible in $Al(CO)_2$, we surmise that essentially all of the back-donation in $Cu(CO)_3$ originates from the semifilled Cu $4p_\pi$ orbital.

Registry No. Cu(CO), 55979-21-0; $Cu(CO)_3$, 55979-19-6.

(15) Kopfermann, H. "Nuclear Moments"; Academic Press: New York, 1958; pp 123-138.
(16) Morton, J. R.; Preston, K. F. *J. Magn. Reson.* **1978**, *30*, 577.
(17) Kasal, P. H.; Jones, P. M. *J. Am. Chem. Soc.* **1984**, *106*, 8018.

NMR Chemical Shift and NMR Isotope Shift Evidence for the Influence of Nonbonded Interactions on Charge Distribution in α,β-Unsaturated Methoxycarbenium Ions

David A. Forsyth,*[1a] Virginia M. Osterman,[1a] and John R. DeMember[1b]

Contribution from the Department of Chemistry, Northeastern University, Boston, Massachusetts 02115, and the Research Laboratories, Polaroid Corporation, Cambridge, Massachusetts 02139. *Received August 13, 1984*

Abstract: ^{13}C NMR chemical shifts and deuterium isotope effects on chemical shifts in α,β-unsaturated methoxycarbenium ions provide evidence regarding the influence of nonbonded interactions on charge distribution. The α,β-unsaturated methoxycarbenium ions exist as *Z* and *E* isomers due to restricted rotation about the C_1–O bond. A 5- to 7-ppm difference between *Z* and *E* isomers at C_3, which are sp^2 carbons remote from the site of structural variation, indicates a difference in polarization of the π-bonded segment. Deuterium substitution in the methyl group of the 1-methoxy-2-cyclohexenyl cation induces an upfield shift at C_3 of the *Z* isomer only. This isotope shift, along with the lack of significant shift differences at C_3 in the analogous hydroxycarbenium ions, shows that the polarization is due to an interaction with the methoxy methyl group. The observations are explicable within the theory of nonbonded interactions.

Introduction

Differences in the thermodynamic stability of cis–trans geometrical isomers of alkenes, as well as conformational preferences in a variety of other systems, have been explained in terms of a combination of nonbonded (long-range) orbital interactions and steric effects.[2] A recent study of energy levels of terminal methyl-substituted butadienes by electron-transmission spectroscopy provided evidence for through-space orbital interactions of methyl groups with the π system.[3] We have previously sug-

(1) (a) Northeastern University. (b) Polaroid Corporation.
(2) (a) Epiotis, N. D. *J. Am. Chem. Soc.* **1973**, *95*, 3087–3096. (b) Epiotis, N. D.; Sarkanen, S.; Bjorkquist, L.; Yates, R. L. *Ibid.* **1974**, *96*, 4075–4084. (c) Epiotis, N. D.; Yates, R. L.; Bernardi, F. *Ibid.* **1975**, *97*, 5961–5968. (d) Epiotis, N. D.; Cherry, W. R.; Shaik, S.; Yates, R.; Bernardi, F. *Top. Curr. Chem.* **1977**, *70*.

0002-7863/85/1507-0818$01.50/0